Influence of epitaxial strain on clustering of iron in $Pb(Fe_{1/2}Nb_{1/2})O_{3}$ thin films

S. A. Prosandeev, I. P. Raevski, S. I. Raevskaya, and H. Chen

Phys. Rev. B **92**, 220419 — Published 28 December 2015

DOI: 10.1103/PhysRevB.92.220419

Influence of epitaxial strain on clustering of iron in Pb($Fe_{1/2}Nb_{1/2}$)O_3 thin films

S. A. Prosandeev,[1,2,*] I. P. Raevski,[2] S. I. Raevskaya,[2] and H. Chen[3]

[1]*Institute of Nanoscience Physics and Physics Department,*
University of Arkansas, Fayetteville, Arkansas 72701, USA
[2]*Research Institute of Physics and Physics Department,*
Southern Federal University, Rostov-on-Don 344090, Russia
[3]*Institute of Applied Physics and Materials Engineering,*
Faculty of Science and Technology, University of Macau, Macau, China

Abstract

It was found recently that multiferroic Pb($Fe_{1/2}Nb_{1/2}$)O_3 (PFN) has a complex crystal structure containing nanoscale regions of Fe ions segregated into chemical clusters. This unusual property may have exciting applications, for instance, in magnetic, electric or magnetoelectric devices, and it definitely has a fundamental significance. However, this challenge will be unclaimed until one can find the way how to control this property. In the present study, we investigate the possibility of using an epitaxial strain for these purposes. We have performed first-principles calculations of the energies of different chemical configurations of PFN for a wide range of the misfit strains. We found that the misfit strain does influence the energy, magnetic moments, crystal shape, ferroelectric and even antiferroelectric polarization of PFN, due to a different response to strain of different chemical configurations. This makes the epitaxial strain one of the most valuable candidates to control the chemical clustering in PFN.

Lead iron niobate $\mathrm{Pb(Fe_{1/2}Nb_{1/2})O_3}$ (PFN) belongs to one of the most actively studied multiferroics possessing simultaneously the ferroelectric (FE) and magnetic orders[1–3]. On cooling, PFN undergoes FE[4–6] and magnetic phase transitions[2,3,6,7], it is supposed to have the FE relaxor-[6,8,9] or even birelaxor-properties[7], while some of them might have extrinsic reasons[10]. First-principles calculations of the energies of different chemical configurations of PFN revealed an unusual effect of Fe nanoscale ordering[11] influencing magnetic properties of PFN[12,13]. In line with these predictions, the studies of Mossbauer-[11] and NMR-spectra[14] showed that PFN is chemically inhomogeneous at nanoscale. Very probably, this evidence can explain the fact that the experimental value of the Neel temperature, $T_N \approx 150\mathrm{K}$, in PFN is much lower than the value estimated on the basis of the random distribution of the Fe and Nb ions in the lattice[15]. Similarly, calculations[11] and experiment[3,16–18] showed that this kind of Fe ordering should take place also in $\mathrm{Pb(Fe_{1/2}Ta_{1/2})O_3}$ (PFT), but, in $\mathrm{Pb(Fe_{1/2}Sb_{1/2})O_3}$ (PFS), one may expect only local crystal structure excitations of this kind. Glinchuk et.al[19] explained unusual magnetic properties of the solid solutions of PFN and PFT with lead zirconium tianate (PZT) by internal pressure in nano droplets of Fe that again supports the idea of Fe-clustering. However, one cannot exclude the possibility of a small admixture of ferromagnetic or ferrimagnetic compounds, like $\mathrm{PbFe_{12}O_{19}}$, in PFN[20].

The self-organization of the Fe ions in PFN under discussion would be of great interest for applications if one could control it. Previously, Li- doping was successfully used to change the degree of the compositional ordering of B-site cations in $\mathrm{Pb(B^{3+}_{1/2}B^{5+}_{1/2})O_3}$ perovskites with $\mathrm{B^{3+}}$ =Sc, Yb and $\mathrm{B^{5+}}$ =Nb, Ta[21,22]. Li-doping was reported to decrease T_N in the PFN and PFT ceramics by about $50\mathrm{K}$[23]. However, it is more important to increase T_N up to near–room temperatures that, probably, can be done if one could increase the disorder of the B-ions in PFN. It was recently reported that high-energy mechanical activation of $\mathrm{Pb(B^{3+}_{1/2}B^{5+}_{1/2})O_3}$ perovskite ceramics increases the disorder of the B-site cations and increases T_N[24,25]. However, further annealing decreased T_N back[25]. Recently, there appeared an intriguing report about T_N values in a PFN thin film of about $200\mathrm{K}$[17]. Moreover, in this film, a remnant magnetization was observed up to room temperature, while, in bulk PFN single crystals, it vanished above $10 - 15\mathrm{K}$[9].

One of the goals of the present study is to investigate the stability of different chemical configurations of Fe in PFN films, from first principles, as a function of the misfit strain, and to characterize these films by calculating their magnetic and FE properties. Another aim is to calculate phase diagrams of the PFN films versus the misfit strain for each of the chemical configurations considered. Note that the calculation of the phase diagrams of thin films versus strain has become rather popular nowadays. For example, such calculations were done within Landau-approach[26], first-principles approaches[27], and effective Hamiltonian method[28,29].

We performed the first-principles calculations within the local spin-density approximation (LSDA+U technique)[30,31] by employing the package for *ab-initio* computations "Vienna ab initio simulation program" (VASP)[32,33]. We used the generalized gradient approximation (GGA) in the form proposed by Perdew, Burke, and Ernzerhof (PBE)[34]. We employed the functional obtained by the Projector augmented-wave (PAW) method[35]. The supercells included 40 ions in the geometry $2 \times 2 \times 2$, in terms of the primitive perovskite ABO_3 structure unit cells. The translation vectors a, b, and c were directed along $[100]$, $[010]$ and $[001]$ main crystallographic axes. Four main chemical configurations, found in Ref.[11], were considered. One is the most symmetric distribution of the Fe and Nb ions with the Rock-Salt $1 : 1$ - type order, which we will denote as configuration (a). The other, configuration (b), is a planar 1:1 distribution of Fe and Nb, with the Fe and Nb atomic planes perpendicular to the substrate. The third configuration, (c), contains the local Fe and Nb clustering discussed in Ref.[11] (to be shown below). At last, but not least, configuration (d) is also planar, as configuration (b), but with the Fe and Nb planes in parallel with the substrate.

The self-consistent calculations of the parameter U responsible for the $d - d$ Coulomb interaction on Fe ions in $BiFeO_3$ gave U equal to 3.8 eV[36], and, in FeO, it is equal to 4.3 eV[37]. Note that the dependence of the stability of different chemical configurations on U in PFN has been already studied earlier[11]. Those results showed that small variations of this parameter do not change significantly the relative energies of the chemical configurations in PFN. This is why, we employed here the value of 4.0 eV discussed in Ref.[11], and we did not study here the change of the results in response to the change of U. The k-point mesh was $4 \times 4 \times 4$ and the cut-off energy for the electrons was 500 eV. The magnetic structure was selected by choosing the minimum of the total energy. Specifically, in all these structures, each Fe spin was antiferromagnetically arranged with respect to the nearest Fe spins, independently of the chemical configuration. Only the most symmetric structure, (a), which did not have nearest-neighbor Fe pairs, had I-type antiferromagnetic structure (the second nearest neighbors have opposite spin projections).

We structurally relaxed all supercells without any symmetry limitation. The epitaxial strain conditions were imposed during the whole calculation via fixing two lattice vectors in the basal plane and by automatic varying only the third lattice vector to minimize the forces. Specifically, we selected the first two vectors as $(a, 0, 0)$ and $(0, a, 0)$, where a is the lattice constant of the substrate, which we supposed to be square-like. The third vector was (u, w, c), with all three quantities, u, w, and c, varied self-consistently until full convergence with the precision of energy $10^{-5}\mathrm{eV}$. The misfit strain was changed from -4.5% to 4.5%.

Fig. 1 presents the dependence of the total energy of the four chemical configurations studied on the misfit strain. One can see that configuration (a) has the highest energy, in the whole range of strain. Three other configurations compete each with the other: at small strain, the planar configurations are of the lowest energy, while, at large compressive strain, configuration (c) dominates. Note that, at this highest compressive strain, the energy difference between different configurations decreases that should make the sample more disordered, and, correspondingly, one may expect increase of T_N, in line with experiment[17].

Additional challenge is to study the crystallographic deformation and magnetic properties of different chemical configurations of PFN versus the misfit strain. Fig. 2(1) presents the c/a ratio as a function of the misfit strain. One can see that all four configurations have similar c/a ratio in the range of the tensile strain (positive values of the misfit strain), but, in the range of the compressive strain, configurations (a) and (d) have larger c/a than configurations (b) and (c). In configuration (a), this increase happens in the way inherent to a phase transition to a supertetragonal phase (note the abrupt change of the c/a ratio in configuration (a) at exactly the same misfit strain as in Fig. 1).

Interestingly, magnetic properties of the four different chemical configurations are also different. As one can see from Fig. 2(2), the average magnitude of the magnetic moment per Fe ion in the planar configuration (d) is the lowest in the compressive strain region, and configuration (b) has the smallest magnetic moment in the tensile strain region. The largest magnetic moment exists in the symmetric configuration (a) in the whole range of strain. It is interesting that this moment abruptly changes (decreases) at the phase transition to the supertetragonal phase, on the increase of the magnitude of the compressive strain.

In order to characterize the results better, we calculated polarization, by using the atomic displacements and calculated by us dynamical charges. The results are shown in Figure 3. For all configurations, three different regions can be selected, which drastically differ by the morphology of the polarization. In region I, we have a tetragonal or quasi-tetragonal structure. We denoted it as c, in line with Pertsev notations[26]. Almost all the electric dipoles, in this phase, look out of plane. Configurations (a), (c), and (d) in region II, have the symmetry of r type, in Pertsev notations[26], which implies that the out-of-plane and in-plane components of polarization are comparable. In configuration (b), this symmetry is of ac type. This unusual symmetry is a consequence of the symmetry of the Nb and Fe planes. In configuration (b), these planes are arranged perpendicular to the substrate. Such arrangement dictates the symmetry of polarization: it is directed along the Nb-and-Fe planes that can be explained by the large electric polarizability of the Nb planes. Thus, by engineering the atomic structure of PFN one can control the direction (and magnitude) of the polarization. Finally, region III, contains mostly the in-plane dipoles. However, there is still some difference between configurations (a), (c), and (d), on the one hand, and (b) on the other: configuration (b) has two different in-plane components (x and y), while configurations (a), (c), and (d) are orthorhombic.

We found the polarization in PFN strongly inhomogeneous. In order to characterize this inhomogeneity, we calculated the antiferroelectric (AFE) polarization: $\mathbf{P}^{AFE}(\mathbf{q}) = \frac{1}{V}\sum_j \mathbf{p}_j e^{i\mathbf{q}\cdot\mathbf{r}_j}$, where $\mathbf{q}$ is the wave vector, V is the volume of the supercell, $\mathbf{p}_j$ is the dipole moment associated with the atomic displacement and calculated with the use of the Berry phases, and $\mathbf{r}_j$ is the atomic centrosymmetric coordinate of the ion. Fig. 4 presents the results of the calculations of this AFE polarization. One can see that this polarization is significant in the whole range of the strain and in all chemical configurations, but the type of this polarization is different. For example, in configuration (a), in the range of tensile strain, the AFE moment is along z, but it switches to (110) direction in the range of compressive strain. The $\mathbf{q}$-vector, in this configurations is $(1/2, 1/2, 1/2)$. Interestingly the value of the AFE polarization for configuration (a) is the largest among the configurations considered. This fact is in line with the well documented data that the $\mathrm{PbB}^{3+}_{1/2}\mathrm{Nb}_{1/2}\mathrm{O}_3$ perovskites are AFE in the highly-ordered state and FE in the disordered state[21,22]. The largest AFE component in configuration (b) is perpendicular to the Nb and Fe planes and has $\mathbf{q}$-vector $(0, 1/2, 0)$. Configuration (c) has a similar AFE polarization, but in all three directions, x, y, and z. At last, configuration (d), which is planar, has AFE polarization perpendicular to the Nb and Fe planes, as in configuration (b). Note that AFE polarization was also found recently in $\mathrm{PbMg}_{1/3}\mathrm{Nb}_{2/3}\mathrm{O}_3$ and $\mathrm{BaZr}_{1/2}\mathrm{Ti}_{1/2}\mathrm{O}_3$ relaxors[38,39].

The results obtained in this study are in good accord with the previous results of other authors on similar objects. For example, it was found theoretically, from first principles[40] and experimentally[41] that the (001) BiFeO_3 thin films change their symmetry from the monoclinic Cc to tetragonal Cm phase under some compressive strain. The phase transition between these two phases is followed by a strong increase of c/a. We found similar situation in all chemical configurations, but only in configuration (a) this phase transformation is abrupt. In contrast to this fact, for example, in Ref.[42], it was found that PZT, under two-dimensional tensile strain, has only in-plane polarization components. We obtained similar results for all chemical configurations of PFN.

We found out that, in PFN, in all chemical configurations, in the whole range of strain, the polarization is locally inhomogeneous, and this inhomogeneity depends on the distribution of the Nb and Fe ions. We characterize this inhomogeneity by the introduction of the AFE polarization. For example, in configuration (a) we found out that this AFE polarization has $(1/2, 1/2, 1/2)$ order. This implies that each dipole, say, on the Pb ions, is surrounded by opposite Pb related dipoles on the nearest neighbor Pb sites. In contrast to this, the other chemical configurations have planar arrangement of the dipoles: one Pb layer has dipoles in one direction and the next Pb layer has oppositely directed dipoles.

We also found that the directions of the largest components of AFE polarization are, in most cases, perpendicular to the direction of polarization. For instance, in configuration (a) at large compressive strain, the polarization is along c, that is perpendicular to the substrate, but the AFE polarization is along $[110]$ direction. In configuration (b), the main component of polarization is along x, while the main component of the AFE polarization is along y. In configurations (c) and (d), at large tensile strain, the polarization is in-plane of the substrate, but the AFE polarization is out of plane. At the same time, in cases (c) and (d), at large compressive strain, both the FE and AFE polarization look out of plane. Thus, besides the ”normal” dependence of the polarization direction on the misfit strain, in PFN, there exists some periodic tilting of polarization, which, very probably, originates from the polarization inhomogeneity of the lead displacements due to their interactions with the FE active Nb ions, because this AFE polarization strongly depends on the chemical configuration considered.

In conclusion, we obtained that the energy difference between different chemical configurations of PFN decreases on the compressive strain. This can make the distribution of the Fe and Nb ions in the lattice more disordered in range I than in range II. Structural and magnetic properties of the films with different chemical order are also different. For example, only configuration (a) shows the abrupt phase transition to the supertetragonal phase that is followed with the jumps of the c/a ratio and average magnetic moment magnitude. On the other hand, the qualitative change in all chemical configurations is similar: the increase of the compressive strain increases c/a ratio and decreases magnetic moment on Fe. The calculated phase diagrams show that some of their details depend on the chemical configuration. For example, region III in configuration (b) has monoclinic FE order, whereas configurations (a), (c), and (d) have orthorhombic order. In region

II, configuration (b) shows orthorhombic FE order, while configurations (a), (c), and (d) are nearly rhombohedral. We have discovered the presence of the AFE order in PFN, and this order proves very dependent on the strain and chemical configuration. The results obtained show that the strain engineering can be successfully used to modify not only FE, AFE, and magnetic properties, but also can change the degree of Fe ordering influencing different characteristics of the multiferroic thin films and superstructures via the change of the chemical order.

This study was partially supported by the Russian Foundation for Basic Research (project 14-02-90438_Ucr_a), Ministry of Education and Science of Russian Federation (research project 2132), and Research Committee of the University of Macau (Research & Development Grant for Chair Professor No RDG007/FST-CHD/2012)

---

* sprossan@uark.edu

[1] D. I. Khomskii, J. Magn. Magn. Mater. **306**, 1 (2006).

[2] W. Kleemann, V. V. Shvartsman, P. Borisov, and A. Kania. Phys. Rev. Lett. **105**,257202 (2010).

[3] R. Blinc, P. Cevc, A. Zorko, J. Holc, M. Kosec, Z. Trontelj, J. Pirnat, N. Dalal, V. Ramachandran, and J. Krzystek, J. Appl. Phys. **101**, 033901 (2007).

[4] K. H. Ehses and H. Schmid, **162**, 64 (1983).

[5] W. Bonny, M. Bonin, Ph. Sciau, K. J. Schenk, and G. Chapuis, Solid State Commun. **102**, 347 (1997).

[6] S. P. Singh, S. M. Yusuf, S. Yoon, S. Baik, N. Shin, and D. Pandey, Acta Mater. **58**, 5381 (2010).

[7] R. Pirc, R. Blinc, and J. F. Scott, Phys. Rev. B **79**, 214114 (2009).

[8] G. M. Rotaru, B. Roessli, A. Amato, S. N. Gvasaliya, C. Mudry, S. G. Lushnikov, and T. A. Shaplygina, Phys. Rev. B. **79**, 184430 (2009).

[9] V. V. Laguta, M. D. Glinchuk, M. Maryško, R. O. Kuzian, S. A. Prosandeev, S. I. Raevskaya, V. G. Smotrakov, V. V. Eremkin, I. P. Raevski, Phys. Rev. B **87**, 064403 (2013).

[10] I. P. Raevski, S. P. Kubrin, S. I. Raevskaya *et al*, IEEE Trans. Ultrason. Ferroelect. Freq. Contr. **59**, 1872 (2012).

[11] I. P. Raevski, S. P. Kubrin, S. I. Raevskaya, D. A. Sarychev, S. A. Prosandeev, and M. A. Malitskaya, Phys. Rev. B. **85**, 224412 (2012).

[12] R. O. Kuzian, I. V. Kondakova, A. M. Daré, and V. V. Laguta, Phys. Rev. B **89**, 024402 (2014).

[13] R. O. Kuzian, V. V. Laguta, and J. Richter, Phys. Rev. B **90**, 134415 (2014).

[14] V. V. Laguta, J. Rosa, L. Jastrabik, R. Blinc, P. Cevc, B. Zalar, M. Remskar, S. I. Raevskaya, and I. P. Raevski, Mater. Res. Bull. **45**, 1720-1727 (2010).

[15] S. Nomura, H. Takabayashi, and T. Nakagawa, Jpn. J. Appl. Phys. **7**, 600 (1968).

[16] D. A. Sanchez, N. Ortega, A. Kumar, G. Sreenivasulu, R. S. Katiyar, J. F. Scott, D. M. Evans, M. Arredondo-Arechavala, A. Schilling, and J. M. Gregg, J. Appl. Phys. **113**, 074105 (2013).

[17] W. Peng, N. Lemee, M. Karkut, B. Dkhil, V. Shvartsman, P. Borisov, W. Kleemann, J. Holc, M. Kosec, and R. Blinc, Appl. Phys. Lett. **94**, 012509 (2009).

[18] V. V. Laguta, V. A. Stephanovich, M. Savinov, M. Marysko, R. O. Kuzian, N. M. Olekhnovich, A. V. Pushkarev, Yu. V. Radyush, I. P. Raevski, S. I. Raevskaya, and S. A. Prosandeev, New J. Phys. **16**, 11304 (2014).

[19] M. D. Glinchuk, E. A. Eliseev, A. N. Morozovska, J. Appl. Phys. **116**, 054101 (2014).

[20] I. P. Raevski, V. V. Titov, M. A. Malitskaya, E. V. Eremin, S. P. Kubrin, A. V. Blazhevich, H. Chen, C.-C. Chou, S. I. Raevskaya, I. N. Zakharchenko, D. A. Sarychev, and S. I. Shevtsova, J. Mater. Sci. **49**, 6459-6466 (2014).

[21] A. A. Bokov, V. Y. Shonov, I. P. Rayevsky, E. S. Gagarina, and M. F. Kupriyanov, J. Phys. Condens. Matter. **5**, 5491 (1993).

[22] I. P. Raevski, V. Yu. Shonov, M. A. Malitskaya, E. S. Gagarina, V. G. Smotrakov, and V. V. Eremkin, Ferroelectrics **235**, 205 (1999).

[23] I. P. Raevski, S. P. Kubrin, S. I. Raevskaya, V. V. Stashenko, D. A. Sarychev, M. A. Malitskaya, M. A. Seredkina, V. G. Smotrakov, I. N. Zakharchenko, and V. V. Eremkin, Ferroelectrics **373**, 121 (2008).

[24] X. Gao, J. Xue, and J. Wang, Mater. Sci. Eng. B. **99**, 63 (2003).

[25] A. A. Gusev, S. I. Raevskaya, V. V. Titov, A. G. Avvakumov, V. P. Isupov, I. P. Raevski, H. Chen, C.-C. Chou, S. P. Kubrin, S. V. Titov, M. A. Malitskaya, A. V. Blazhevich, D. A. Sarychev, V. V. Stashenko, and S. I. Shevtsova, Ferroelectrics. **475**, 41 (2015).

[26] N. A. Pertsev, V. G. Kukhar, H. Kohlstedt, and R. Waser, Phys. Rev. B **67**, 054107 (2003).

[27] O. Dieguez, S. Tinte, A. Antons, C. Bungaro, J. B. Neaton, K. M. Rabe, and D. Vanderbilt, Phys. Rev. B **69**, 212101 (2004).

[28] B.-K. Lai, I. A. Kornev, L. Bellaiche, and G. J. Salamo, Appl. Phys. Lett. **86**, 132904 (2005).

[29] S. Prosandeev, D. Wang, L. Bellaiche, Phys. Rev. Lett. **111**, 247602 (2013).

[30] V. I. Anisimov, F. Aryasetiawan, and A. I. Lichtenstein, J. Phys.: Condens. Matter **9**, 767 (1997).

[31] G. Kresse and J. Hafner, Phys. Rev. B **47**, 558R (1993); G. Kresse and J. Furthmuller, *ibid.* **54**, 11169

(1996).

[32] G. Kresse and J. Hafner, Phys. Rev. B 47, 558 (1993); *ibid.* 49, 14251 (1994).

[33] G. Kresse and J. Furthmüller, Comput. Mater. Sci. 6, 15 (1996); Phys. Rev. B 54, 11169 (1996).

[34] J. P. Perdew, K. Burke, and M. Ernzerhof, Phys. Rev. Lett. **77**, 3865 (1996).

[35] P. E. Bl"ochl, Phys. Rev. B **50**, 17953 (1994).

[36] D. Albrecht, S. Lisenkov, W. Ren, D. Rahmedov, I. A. Kornev, and L. Bellaiche, Phys. Rev. B **81**, 140401(R) (2010).

[37] M. Cococcioni and S. de Gironcoli, Phys. Rev. B **71**, 035105 (2005).

[38] S. Prosandeev, D. Wang, A. R. Akbarzadeh, and L. Bellaiche, J. Phys.: Condens. Matter **27**, 223202 (2015).

[39] A. Al-Barakaty, S. Prosandeev, D. Wang, B. Dkhil, and L. Bellaiche, Phys. Rev. B **91**, 214117 (2015).

[40] B. Dupé, I. C. Infante, G. Geneste, P.-E. Janolin, M. Bibes, A. Barthélémy, S. Lisenkov, L. Bellaiche, S. Ravy, and B. Dkhil, Phys. Rev. B **81**, 144128 (2010).

[41] H. Béa, B. Dupé, S. Fusil, R. Mattana, E. Jacquet, B. Warot-Fonrose, F. Wilhelm, A. Rogalev, S. Petit, V. Cros, A. Anane, F. Petroff, K. Bouzehouane, G. Geneste, B. Dkhil, S. Lisenkov, I. Ponomareva, L. Bellaiche, M. Bibes, and A. Barthélémy, Phys. Rev. Lett. **102**, 217603 (2009).

[42] P.-E. Janolin, N. A. Pertsev, D. Sichuga, and L. Bellaiche, Phys. Rev. B **85**, 140401(R) (2012).

Captions

Fig.1. Dependence of the total energy of the four chemical configurations in PFN on the misfit strain. The insets show the crystal structure for the chemical configurations studied.

Fig. 2. Dependence of the c/a ratio (1) and average magnetic moment (2) on the misfit strain in different chemical configurations of PFN.

Fig. 3. Polarization of PFN thin film vs misfit strain calculated for four different configurations of Fe and Nb cations. The symmetry is denoted by using Pertsev notations[26].

Fig. 4. AFE Polarization in PFN thin film vs misfit strain calculated for four different chemical configurations.

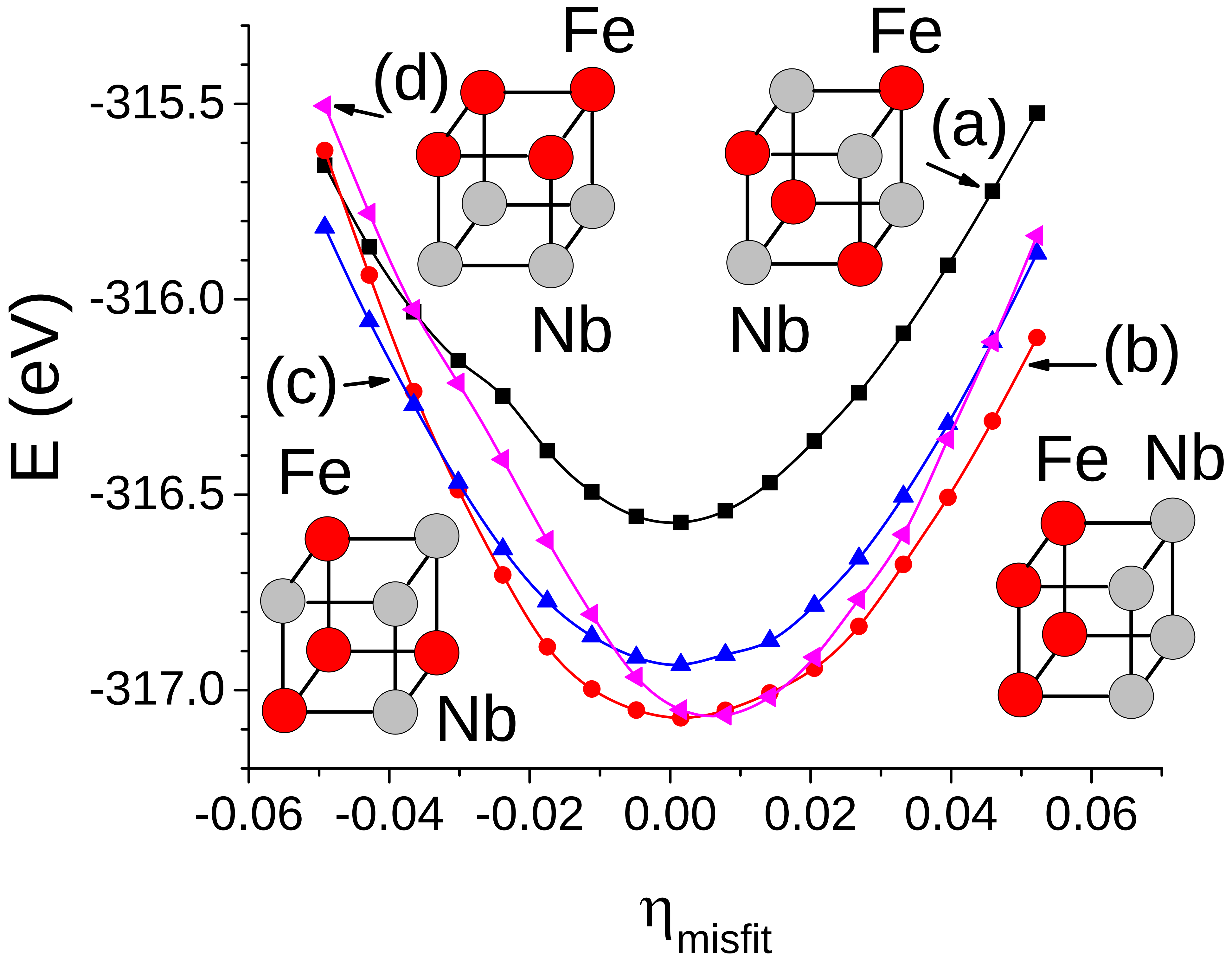
Fe
Fe
(d)
(a)
Nb
Nb
(c)
(b)
Fe
Fe Nb
Nb
E (eV)
-315.5
-316.0
-316.5
-317.0
-0.06
-0.04
-0.02
0.00
0.02
0.04
0.06
η_{misfit}

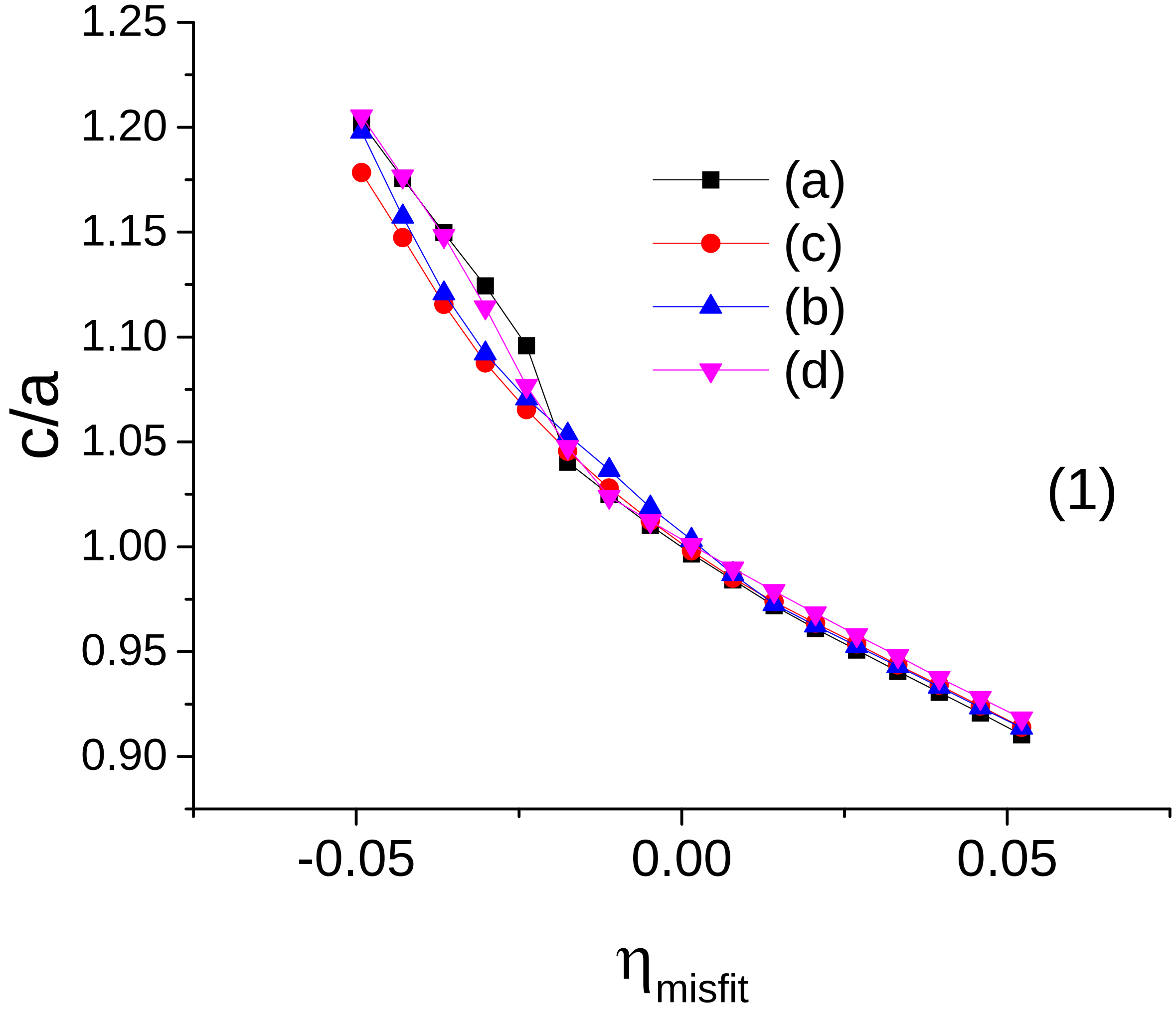
1.25
1.20
1.15
1.10
1.05
1.00
0.95
0.90
c/a
-0.05
0.00
0.05
η_{misfit}
■ (a)
● (c)
▲ (b)
▼ (d)
(1)

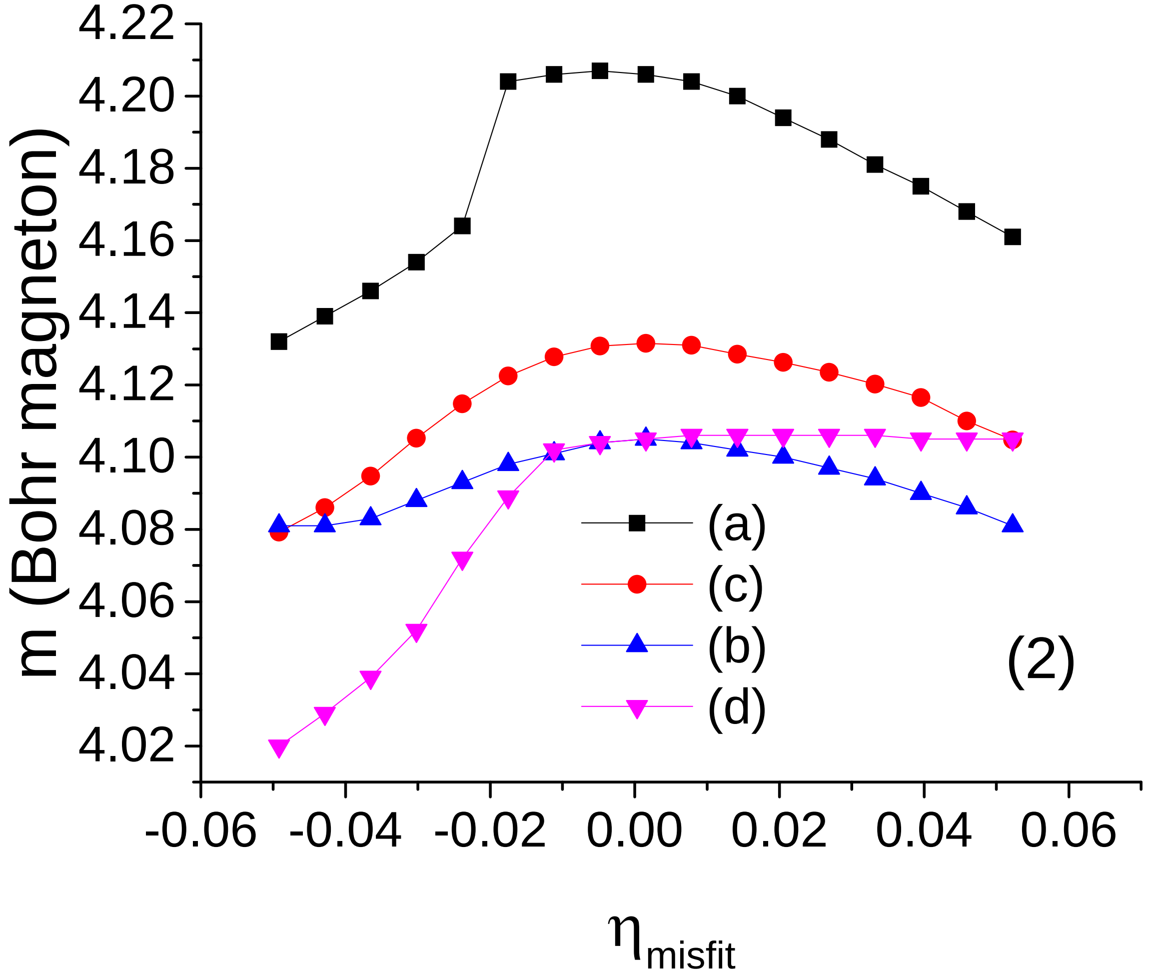
4.22
4.20
4.18
4.16
4.14
4.12
4.10
4.08
4.06
4.04
4.02
m (Bohr magneton)
-0.06
-0.04
-0.02
0.00
0.02
0.04
0.06
η_{misfit}
■ (a)
● (c)
▲ (b)
▼ (d)
(2)

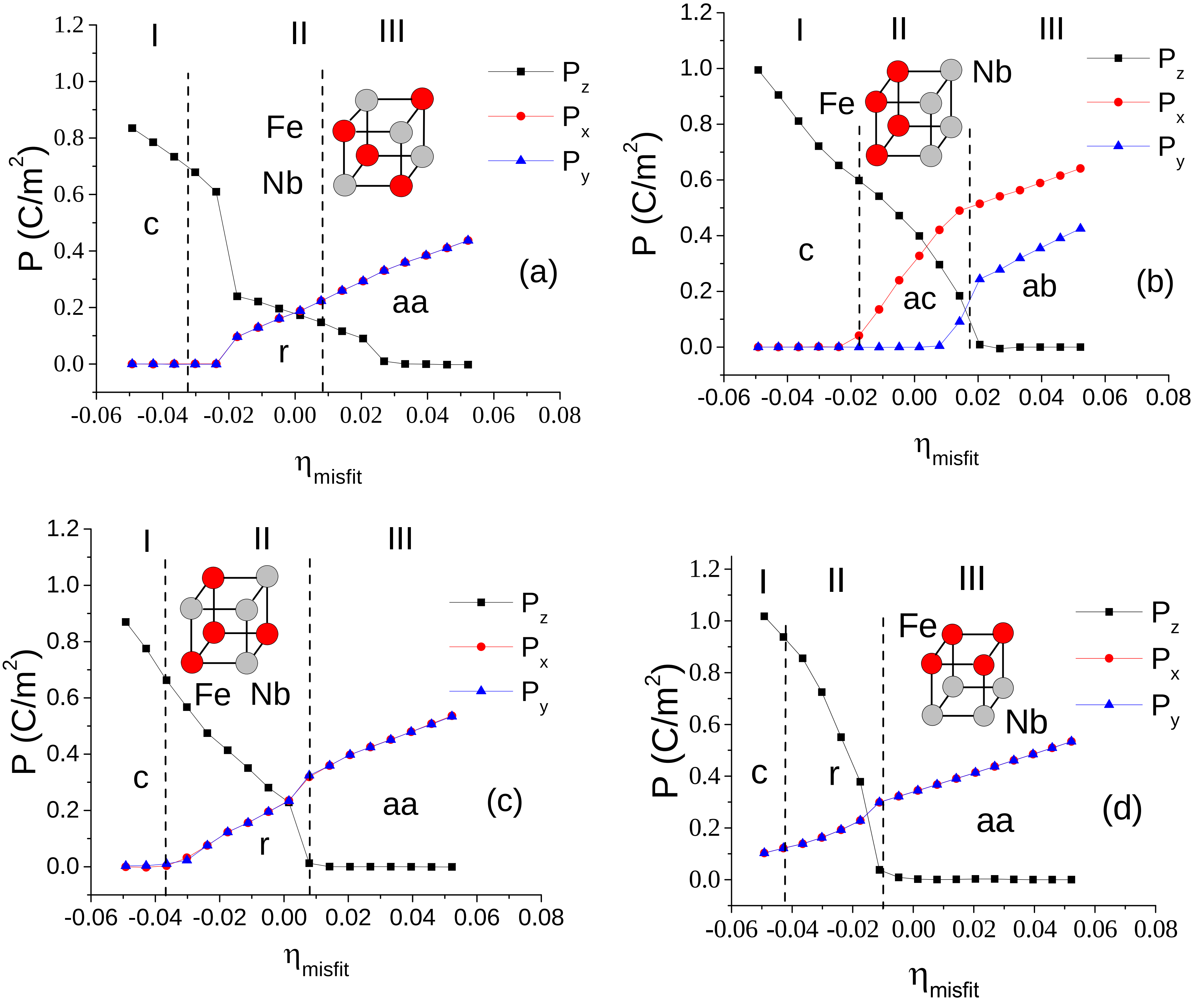
P (C/m^2)
η_{misfit}
I
II
III
c
r
aa
ac
ab
Fe
Nb
P_z
P_x
P_y
(a)
(b)
(c)
(d)
0.0
0.2
0.4
0.6
0.8
1.0
1.2
-0.06
-0.04
-0.02
0.00
0.02
0.04
0.06
0.08

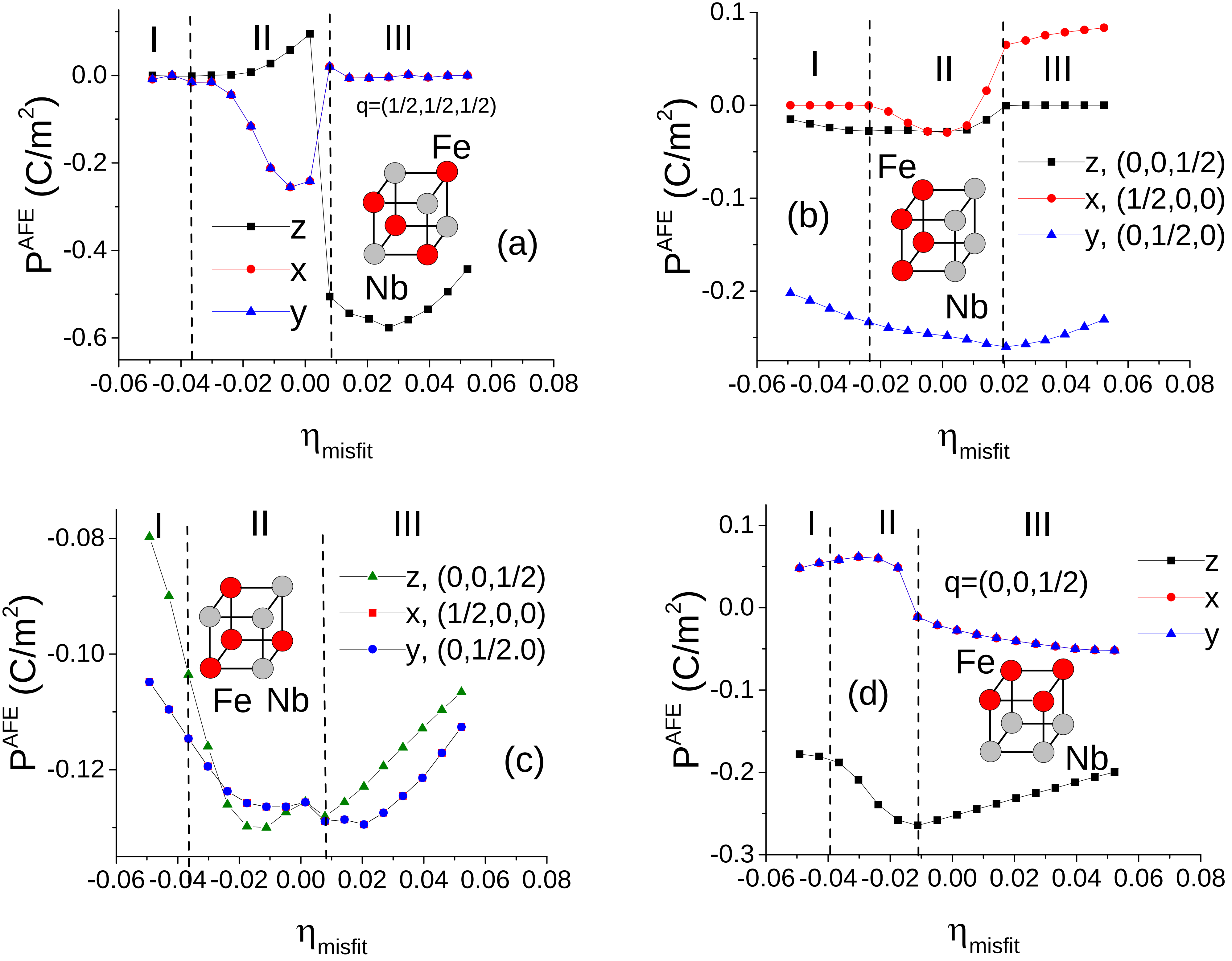

(a)
I
II
III
q=(1/2,1/2,1/2)
Fe
Nb
z
x
y
P^{AFE} (C/m^2)
0.0
-0.2
-0.4
-0.6
-0.06 -0.04 -0.02 0.00 0.02 0.04 0.06 0.08
η_{misfit}
(b)
I
II
III
Fe
Nb
z, (0,0,1/2)
x, (1/2,0,0)
y, (0,1/2,0)
P^{AFE} (C/m^2)
0.1
0.0
-0.1
-0.2
-0.06 -0.04 -0.02 0.00 0.02 0.04 0.06 0.08
η_{misfit}
(c)
I
II
III
Fe Nb
z, (0,0,1/2)
x, (1/2,0,0)
y, (0,1/2.0)
P^{AFE} (C/m^2)
-0.08
-0.10
-0.12
-0.06 -0.04 -0.02 0.00 0.02 0.04 0.06 0.08
η_{misfit}
(d)
I
II
III
q=(0,0,1/2)
Fe
Nb
z
x
y
P^{AFE} (C/m^2)
0.1
0.0
-0.1
-0.2
-0.3
-0.06 -0.04 -0.02 0.00 0.02 0.04 0.06 0.08
η_{misfit}